

EMPIRICAL MODE DECOMPOSITION, FRACTIONAL GAUSSIAN NOISE AND HURST EXPONENT ESTIMATION

Gabriel Rilling^(*), Patrick Flandrin^(*) and Paulo Gonçalves^(**)

(*) Laboratoire de Physique (UMR CNRS 5672), École Normale Supérieure de Lyon
46, allée d'Italie 69364 Lyon Cedex 07, France
gabriel.rilling@ens-lyon.fr, flandrin@ens-lyon.fr

(**) INRIA Rhône-Alpes

On leave at IST-ISR, Av. Rovisco Pais, 1049-001 Lisbon, Portugal
Paulo.Goncalves@inria.fr

ABSTRACT

Huang's data-driven technique of Empirical Mode Decomposition (EMD) is applied to the versatile, broadband, model of fractional Gaussian noise (fGn). The spectral analysis and statistical characterization of the obtained modes reveal an equivalent filter bank structure together with Gamma distributed variances, both sharing some properties with wavelet decompositions. These common features are then used to mimic wavelet based techniques aimed at estimating the Hurst exponent.

1. INTRODUCTION

Empirical Mode Decomposition (EMD) has been recently pioneered by Huang *et.al.* [1, 2] for adaptively decomposing nonstationary and/or nonlinear time series. More recently, its application to some broadband processes has been shown to spontaneously achieve wavelet-like decompositions [3, 4]. In this paper, we explore further this striking feature by evaluating the potential usefulness of this technique for estimating scaling exponents. New EMD-based methods are proposed and quantitatively compared to classical wavelet-based ones.

2. EMD BASICS

Basically, Empirical Mode Decomposition (EMD) [1] considers a signal at the scale of its local oscillations. The main idea of EMD is then to formalize the idea that, locally: "signal = fast oscillations superimposed to slow oscillations". Looking at one local oscillation (defined, e.g., as the signal between two consecutive local minima), EMD is designed to define a local "low frequency" component as the *local trend* that supports a local "high frequency" component as a zero-mean oscillation or *local detail* so that we can express $x(t)$ as:

$$x(t) = m_1[x](t) + d_1[x](t), \quad (1)$$

with $m_1[x](t)$ corresponding to the *local trend* and $d_1[x](t)$ to the *local detail*. By construction, $d_1[x](t)$ is an oscillatory signal and, if it is furthermore required to be locally zero-mean everywhere, it corresponds to what is referred to as an *Intrinsic Mode Function* (IMF). Practically, this mostly implies that all its maxima are positive and all its minima negative. On the other hand,

all we know about $m_1[x](t)$ is that it locally oscillates slower than $d_1[x](t)$. We can then apply the same decomposition to it, leading to: $m_1[x](t) = m_2[x](t) + d_2[x](t)$ and, recursively applying this on the $m_k[x](t)$, we get a representation of $x(t)$ of the form:

$$x(t) = m_K[x](t) + \sum_{k=1}^K d_k[x](t). \quad (2)$$

At each step of the decomposition, we can state that $d_{k+1}[x](t)$ contains approximatively as many oscillations as $m_k[x](t)$. Correspondingly, $m_{k+1}[x](t)$ (and so $d_{k+2}[x](t)$) contains less, and locally slower, oscillations than $m_k[x](t)$ (and so $d_{k+1}[x](t)$). The decomposition usually ends when the signal $m_K[x](t)$ does not contain enough oscillations to define a meaningful local trend. EMD performs thus a multi-scale decomposition that is fully data-driven and that can be applied to all oscillatory time series, including nonstationary ones and/or those generated by a nonlinear system.

Given a signal $x(t)$, the effective EMD algorithm is given by the following loop [1]:

1. identify all extrema of $x(t)$
2. interpolate between minima (resp. maxima), ending up with some "envelope" $e_{min}(t)$ (resp. $e_{max}(t)$)
3. compute the *local trend* $m(t) = \frac{(e_{min}(t) + e_{max}(t))}{2}$
4. extract the *local detail* $d(t) = x(t) - m(t)$
5. iterate on the residual $m(t)$

In practice, the above procedure has to be refined by a *sifting* process, an inner loop that iterates steps 1 to 4 upon the detail signal $d(t)$, until this latter can be considered as zero-mean according to some stopping criterion¹.

3. EMD ANALYSIS OF FRACTIONAL GAUSSIAN NOISE

3.1. The model of fractional Gaussian noise

Fractional Gaussian noise (fGn) is a generalization of ordinary discrete white Gaussian noise, and it is a versatile model for broadband noise dominated by no particular frequency band. The fGn

¹The effective algorithm used in this study can be found together with some examples at <http://perso.ens-lyon.fr/patrick.flandrin/emd.html>

of parameter H (referred to as the Hurst exponent) can be defined as the only zero-mean stationary Gaussian process with autocorrelation sequence $r_H[k] := \mathbb{E}\{x_H[n]x_H[n+k]\}$ [5]:

$$r_H[k] = \frac{\sigma^2}{2} \left(|k-1|^{2H} - 2|k|^{2H} + |k+1|^{2H} \right). \quad (3)$$

As it is well-known, the case $H = \frac{1}{2}$ reduces to discrete white noise. For all H , we can approximate the power spectrum density of fGn by $S_H(f) \sim C\sigma^2|f|^{1-2H}$ when $|f| \rightarrow 0$, making of fGn a convenient model for power-law spectra at low frequencies. In fact, it has to be noted that the approximation is fairly well verified over most of the Nyquist frequency band.

3.2. Filter bank structure

Following upon the preliminary findings reported in [3], we carried out extensive numerical simulations on fGn processes, with $H = 0.1, 0.2, \dots, 0.9$. For each value of H , $J = 10000$ independent fGn sequences of length $N = 2048$ have been generated via the Wood and Chan algorithm [6], resulting in a collection of IMFs. Although the number of IMFs depends on the realization, all of them ended up with at least 8 modes. Therefore, we will only consider the first 8 IMFs in the study.

Given this data set, a spectral analysis has been carried out mode by mode, using an ensemble average over the J realizations of a classical, correlation based, power spectrum density estimate (see Figure 1). First, it appears that EMD presents two distinct behaviors depending on the value of H . For $H < 0.5$, some of the IMFs seem to act as active filters amplifying the lower frequency band. This implies also that IMFs of different indexes must be strongly correlated. This amplification behavior contradicts the idea of EMD as a *decomposition* as the frequency contents of different modes compensate each other when they are summed to get back the original fGn. Taking this into account, the EMD analysis of mostly high-pass signals should be taken very carefully. Indeed, some low frequency contents might appear in the decomposition although it is not in the analyzed signal. Therefore, to avoid bad intuitions, it would be more accurate to think of EMD as a *transform* when the analyzed signal contains mostly high frequencies. On the contrary, for $H > 0.5$, all filters are passive and their maximum gain does not depend on the index. In this case, the IMFs are far less correlated. Whatever the value of H , the behavior of the first IMF contrasts with that of the others in the sense that it presents the characteristics of a high-pass signal, while the others look much more band-pass. This high-pass behavior has however to be tempered by the fact that the attenuation in the stop-band is no more than 10 dB, thus corresponding to a non-negligible contribution in the lower half-band in the case $H < 0.5$.

For the indices $k = 2, \dots, 8$ corresponding to band-pass IMFs, the spectra all look quite the same, up to some shifts in abscissa and ordinate, in a surprising reminiscence of what is currently observed in wavelet decompositions. As for the latter, we can check for self-similarity in the “filter bank” structure leading to the scale relation:

$$S_{k',H}(f) = \rho_H^{\alpha_H(k'-k)} S_{k,H}(\rho_H^{k'-k} f) \quad (4)$$

for $2 \leq k, k' \leq 8$ and some parameters α_H and ρ_H . As a consequence, the spectra of the IMFs should collapse onto a single curve, when properly renormalized. This can be observed in the lower part of Figure 1 with the specific choices $\rho_H = 2$ and $\alpha_H = 2H - 1$. As described in [4], the choice of ρ_H can be

refined to get better results. Nevertheless, we will use this simple value because the precise one depends on the effective implementation of the EMD algorithm. However, it is worth stressing the fact that the refined value is always increasing with H .

In the case $H > 0.5$, even if some low frequency discrepancies can be observed, these graphs support the idea that EMD on fGn acts as a dyadic filter bank of constant-Q band-pass filters. When $H < 0.5$, the result is a bit different. If EMD still acts as a dyadic filter bank, the associated filters are not band-pass and the superimposition of the spectra is not as well checked because of some discrepancies in amplitude.

Assuming that relation (4) is effective for any H , we can easily derive the two following relations between the variances of the modes $V_H[k]$, the modes indices k and their mean period $\bar{T}_H[k]$:

$$V_H[k] = C\rho_H^{2(H-1)k} = C2^{2(H-1)k}; \quad (5)$$

$$V_H[k] = C'(\bar{T}_H[k])^{2(H-1)}, \quad (6)$$

this last relation being derived from (5) assuming that $\bar{T}_H[k'] = \rho_H^{k'-k}\bar{T}_H[k]$ for $2 \leq k, k' \leq 8$, which is a natural consequence of the self similar structure of the decomposition.

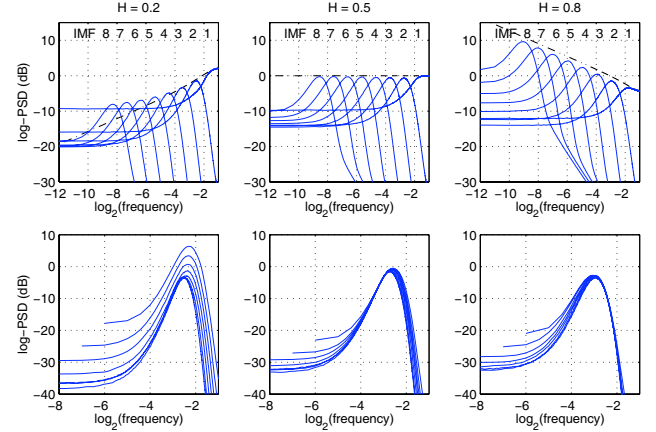


Fig. 1. *Top row:* Mean spectra of the first 8 IMFs and theoretical spectrum of the fGn (dash-dot). The IMFs spectra for $H = 0.2$ rise above the fGn spectrum indicating an amplification. *Bottom row:* Renormalized spectra according to (4).

3.3. Variance distributions

An experimental evidence of relations (5) and (6) is reported in Figure 2 which presents the classical empirical variance estimate

$$\hat{V}_H[k] := \frac{1}{N} \sum_{n=1}^N (d_{k,H}[n])^2 \quad (7)$$

as a function of the mode index k in a semi-log plot and of an empirical (zero-crossing based) estimation of the mean period (8)

$$\hat{T}_H[k] := \frac{\text{distance between the first and the last zero-crossing}}{\text{number of zero-crossings} - 1} \quad (8)$$

in a log-log plot. It can be seen on both diagrams that a straight line can be fitted to all curves for IMF indices $k > 1$, in accordance

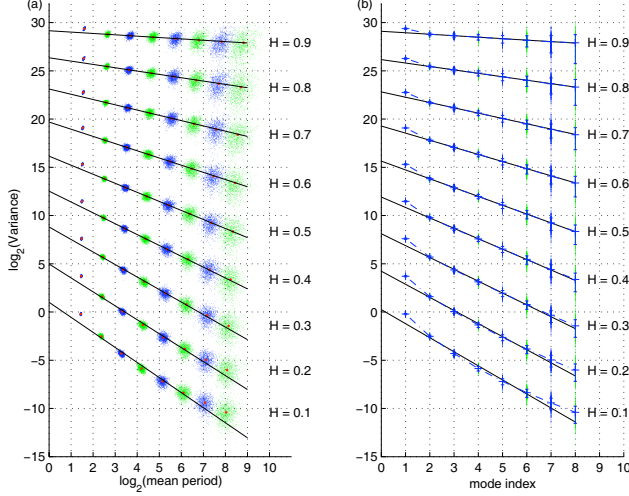


Fig. 2. Simulation results: (a) relation between $V_H[k]$ and $\hat{T}_H[k]$. (b) relation between $V_H[k]$ and the mode index.

with relations (5) and (6). As before, whereas the fit is reasonable for large values of H , it is less significant for $H \leq 0.3$.

To progress further in the study of the variance properties of the IMFs, we will now establish the associated distribution functions. First, let us remind, as reported in [4], that the IMFs associated with fGn of indices $k > 1$ are in fact stationary zero-mean Gaussian processes. As it is well-known, the energy of a zero-mean unit variance stationary independent Gaussian time series of length N has a chi-square distribution with N degrees of freedom. More generally, the energy of such a time series dilated by a scalar factor σ has a Gamma distribution with parameters α and β :

$$P(X = x) \propto x^{\alpha-1} e^{-\frac{x}{\beta}}, \text{ with } \alpha = N/2 \text{ and } \beta = 2\sigma^2. \quad (9)$$

Therefore, the distribution of the energy-based variance estimate (7) of the last process is Gamma with parameters $\alpha = N/2$ and $\beta = 2\sigma^2/N$. There seems to be no such result for an arbitrary correlated stationary Gaussian time series. However, extending the results obtained by Wu *et al.* [7] in the case of white noise, our experiments show that the variance distributions of the IMFs associated with fGn have a Gamma distribution too. An evidence of this behavior is reported in Figure 3 for 3 representative values of H . Moreover, these results have been validated by Kolmogorov–Smirnov tests in almost all cases, for values $0.1 \leq H \leq 0.9$. The latter modelings result in a series of Gamma density parameters which will be referred to as $\alpha_H[k]$ and $\beta_H[k]$ in the following.

4. EMD-BASED ESTIMATION OF HURST EXPONENT

4.1. Construction of the estimators

Based on the above results, we propose two estimators of the Hurst exponent, based either on (5) or on (6): given a self-similar signal $x(t)$ with Hurst exponent H , we compute its EMD and, using the estimates of the variances and mean periods of the associated IMFs $\hat{V}[k]$ (7) and $\hat{T}[k]$ (8), we define the estimator \hat{H}_1 (resp. \hat{H}_2) based on the slope value of a linear fit on the linear part (indices $2 \leq k \leq 8$) of the diagram $\log_2 \hat{V}[k]$ vs. k (resp. $\log_2 \hat{V}[k]$

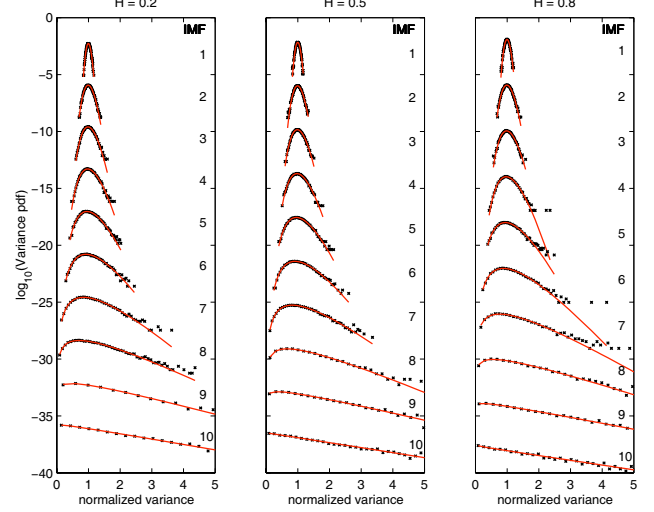


Fig. 3. Variance distributions of the IMFs and fit with Gamma density. For a sake of readiness, the curves have been shifted in ordinates and scaled in abscissa to have a unit mean.

vs. $\log_2 \hat{T}[k]$). In both cases, the fits are obtained through the minimization of a weighted least squares merit function:

$$\hat{H}_1 : \sum_{k=2}^8 \frac{(\log_2 \hat{V}[k] - a_1 k - b_1)^2}{\sigma_V^H[k]^2}; \quad (10)$$

$$\hat{H}_2 : \sum_{k=2}^8 \frac{(\log_2 \hat{V}[k] - a_2 \log_2 \hat{T}[k] - b_2)^2}{\sigma_V^H[k]^2 + a_2^2 \sigma_T^H[k]^2}, \quad (11)$$

where $\sigma_V^H[k]^2$ (resp. $\sigma_T^H[k]^2$) stands for the variance of $\log_2 V_H[k]$ (resp. $\log_2 \hat{T}_H[k]$), and $a_1 k + b_1$ (resp. $a_2 \log_2 \hat{T}[k] + b_2$) for the fitting polynomial for \hat{H}_1 (resp. \hat{H}_2). Assuming relations (5) and (6) to hold, the slopes of the polynomials minimizing (10) and (11) should then verify $a_1^{min} = a_2^{min} = 2(H - 1)$, thus leading to the proposed estimators: $\hat{H}_1 = 1 + a_1^{min}/2$ and $\hat{H}_2 = 1 + a_2^{min}/2$.

Assuming that the distributions of $V_H[k]$ are Gamma, it can be proved that the so-built estimators are in fact biased. More precisely, for a random variable X that has a Gamma distribution with parameters α and β , we can express the expected value of its base 2 logarithm as follows:

$$\mathbb{E} \log_2 X = \log_2 \mathbb{E} X + c(\alpha), \text{ with } c(\alpha) = \frac{\psi(\alpha)}{\ln(2)} - \log_2(\alpha) \quad (12)$$

where $\psi(z) = \Gamma'(z)/\Gamma(z)$ is the Psi function. Taking the latter into account, we can easily define unbiased estimators of the Hurst exponent with the same procedure as described above by replacing $\log_2 \hat{V}[k]$ with $\log_2 \hat{V}[k] - c(\alpha_H[k])$, thus resulting in the merit functions:

$$\hat{H}_1 : \sum_{k=2}^8 \frac{(\log_2 \hat{V}[k] - c(\alpha_H[k]) - a_1 k - b_1)^2}{\sigma_V^H[k]^2} \quad (13)$$

$$\hat{H}_2 : \sum_{k=2}^8 \frac{(\log_2 \hat{V}[k] - c(\alpha_H[k]) - a_2 \log_2 \hat{T}[k] - b_2)^2}{\sigma_V^H[k]^2 + a_2^2 \sigma_T^H[k]^2} \quad (14)$$

estimator	DWT	EMD \hat{H}_1	EMD \hat{H}_2
$H = 0.1$	-0.011± 0.031	0.25±0.037	0.19 ±0.042
$H = 0.2$	0.15 ± 0.03	0.31±0.037	0.26±0.04
$H = 0.3$	0.28 ± 0.031	0.38±0.037	0.34±0.04
$H = 0.4$	0.4 ± 0.03	0.46±0.038	0.43±0.04
$H = 0.5$	0.51 ± 0.03	0.54±0.037	0.53±0.04
$H = 0.6$	0.62 ± 0.03	0.63±0.039	0.63±0.041
$H = 0.7$	0.72 ± 0.03	0.73±0.039	0.73±0.041
$H = 0.8$	0.82 ± 0.031	0.82±0.042	0.83±0.042
$H = 0.9$	0.92 ± 0.031	0.92±0.043	0.93±0.042

Table 1. Expected values and standard deviations of the estimators (“expected value ± standard deviation”). For each H , we highlighted the best values.

estimator	DWT	EMD \hat{H}_1	EMD \hat{H}_2
$H = 0.1$	0.013	0.024	0.01
$H = 0.2$	0.0034	0.014	0.0055
$H = 0.3$	0.0013	0.0078	0.0035
$H = 0.4$	0.00093	0.0048	0.0027
$H = 0.5$	0.001	0.0033	0.0024
$H = 0.6$	0.0012	0.0025	0.0023
$H = 0.7$	0.0013	0.0022	0.0023
$H = 0.8$	0.0015	0.0022	0.0025
$H = 0.9$	0.0015	0.0024	0.0025

Table 2. Mean square errors of the estimators ($bias^2 + variance$). For each H , we highlighted the best value.

It has to be noted that the above procedure assumes some knowledge about H in the definition of the merit functions, namely $\sigma_V^H[k]^2$, $\sigma_T^H[k]^2$ and $c(\alpha_H[k])$. This drawback can be overcome by considering a 2-step procedure:

1. make a coarse estimation of H by minimizing the merit function (13) (resp. (14)) using average values for $\sigma_V^H[k]^2$, $\sigma_T^H[k]^2$ and $c(\alpha_H[k])$, resulting in an estimated value \hat{H} taken as the nearest in the set $0.1, 0.2, \dots, 0.9$.
2. make a finer estimation by minimizing (13) (resp. (14)) using $\sigma_V^{\hat{H}}[k]^2$, $\sigma_T^{\hat{H}}[k]^2$ and $c(\alpha_{\hat{H}}[k])$, resulting in the final estimate \hat{H}_1 (resp. \hat{H}_2).

4.2. Results and comparison with wavelets

The above defined estimators have been tested on 5000 fGn realizations of size $N = 2048$ and for $H = 0.1, 0.2, \dots, 0.9$, together with an estimator based on Discrete Wavelet Transform (DWT) [8]. To compare evenly the DWT and EMD based estimators, we decided to exploit the same range of scales in both cases. Because of the dyadic filter bank structure of EMD, the modes indices are in fact equivalent to the scale indices (or octaves) of the DWT. The results presented here (Tables 1 and 2) are based on the octaves/modes 2 to 7. For all the values of H , we estimated the expected value, the standard deviation and the mean square error of each estimator.

Generally, it turns out that the DWT based estimator overperforms the EMD ones. More precisely, its standard deviation is always the lowest and so is its bias with the noticeable exception of the value $H = 0.1$. For that value, the EMD \hat{H}_2 estimator low bias even allows it to get the lowest mean square error despite

its higher standard deviation. The better achievement of the EMD estimator \hat{H}_2 is mainly due to the great bias of the DWT based estimator. The latter may be linked to the fact that the approximation sequence at scale 0 is generally identified with the analyzed time series. However, for time series with a significant high frequency content, the discrepancy between the two latter may be more important. This is precisely the case involved for a fGn with $H = 0.1$. In fact, the DWT based estimator used in the present study contains a procedure trying to correct this discrepancy but it does not seem to improve meaningfully the results. Finally, the EMD estimators have the drawback that they require an evaluation of the three parameters $\alpha_H[k]$, $\sigma_V^H[k]^2$ and $\sigma_T^H[k]^2$ which depends on the length of the analyzed time series while the DWT based estimator is self-sufficient.

5. CONCLUSION

Although based on no a priori, the EMD method applied to broadband noise reveals a wavelet-like decomposition structure. As for the latter, the variance distributions are Gamma too. These two common properties allowed us to propose new EMD-based estimators of Hurst exponent. The behavior of the two methods (EMD and wavelets) proved to be similar when $H > 1/2$. In the case where $H < 1/2$, our study revealed that the dyadic filter bank structure which underlies the EMD approach is only an approximation that has to be refined further.

Acknowledgement: The authors gratefully acknowledge Patrice Abry (CNRS-ENS Lyon) for fruitful discussions and his help in accurately using wavelet-based estimators.

6. REFERENCES

- [1] N.E. Huang, Z. Shen, S.R. Long, M.L. Wu, H.H. Shih, Q. Zheng, N.C. Yen, C.C. Tung, and H.H. Liu, “The Empirical Mode Decomposition and Hilbert spectrum for nonlinear and non-stationary time series analysis,” *Proc. Roy. Soc. London A*, vol. 454, pp. 903–995, 1998.
- [2] N.E. Huang and S.S.P. Shen, Eds., *Hilbert–Huang Transforms: Introduction and Applications*, World Scientific, 2004, (to appear).
- [3] P. Flandrin G. Rilling and P. Gonçalvès, “Empirical Mode Decomposition as a filter bank,” *IEEE Sig. Proc. Lett.*, vol. 11, no. 2, pp. 112–114, 2004.
- [4] P. Flandrin and P. Gonçalvès, “Empirical Mode Decompositions as a data-driven wavelet-like expansions,” *Int. J. of Wavelets, Multires. and Info. Proc.*, 2004, (to appear).
- [5] P. Embrechts and M. Maejima, *Selfsimilar processes*, Princeton University Press, 2002.
- [6] A.T. Wood and G. Chan, “Simulation of stationary processes in $[0, 1]^d$,” *J. Comp. Graph. Stat.*, vol. 3, pp. 409–432, 1994.
- [7] Z. Wu and N.E. Huang, “A study of the characteristics of white noise using the Empirical Mode Decomposition method,” *Proc. Roy. Soc. London A*, vol. 460, pp. 1597–1611, 2004.
- [8] P. Abry, P. Flandrin, M.S. Taquq, and D. Veitch, “Wavelets for the analysis, estimation and synthesis of scaling data,” in *Self-Similar Network Traffic and Performance Evaluation*, K. Park and W. Willinger, Eds. 2000, pp. 39–88, Wiley.